Direct activation of zebrafish neurons by ultrasonic stimulation revealed by whole CNS calcium imaging

To cite this article before publication: Nicolo Meneghetti *et al* 2020 *J. Neural Eng.* in press https://doi.org/10.1088/1741-2552/abae8b

IOP Publishing Journal Title
Journal **XX** (XXXX) XXXXXX https://doi.org/XXXX/XXXX

Direct activation of zebrafish neurons by ultrasonic stimulation revealed by whole CNS calcium imaging

N. Meneghetti[1,2,+], F. Dedola[1,2,+], V. Gavryusev[3,4,+], G. Sancataldo[4,5], L. Turrini[3,4], G. de Vito[4,6], N. Tiso[7], F. Vanzi[4,8], J. Carpaneto[1,2], A. Cutrone[1,2], F. Saverio Pavone[3,4,9], S. Micera[1,2,10], A. Mazzoni[1,2]

[1] The Biorobotics Institute, Scuola Superiore Sant'Anna, 56025 Pisa, Italy
[2] Department of Excellence for Robotics and AI, Scuola Superiore Sant'Anna, 56025 Pisa, Italy
[3] Department of Physics and Astronomy, University of Florence, 50019 Sesto Fiorentino, Italy
[4] European Laboratory for Non-Linear Spectroscopy (LENS), 50019 Sesto Fiorentino, Italy
[5] Department of Physics and Chemistry, University of Palermo, 90128 Palermo, Italy
[6] Department of Neuroscience, Psychology, Drug Research and Child Health, University of Florence, 50139 Florence, Italy
[7] Department of Biology, University of Padova, 35131 Padova, Italy
[8] Department of Biology, University of Florence, 50019 Sesto Fiorentino, Italy
[9] National Institute of Optics, National Research Council, Florence, Italy
[10] Bertarelli Foundation Chair in Translational Neuroengineering, Center for Neuroprosthetics and Institute of Bioengineering, School of Engineering, École Polytechnique Federale de Lausanne, Switzerland
[+]these authors share same first author contribution

E-mail: a.mazzoni@santannapisa.it

Received xxxxxx Accepted for publication xxxxxx Published xxxxxx

Abstract

Objective: Ultrasounds (US) use in neural engineering is so far mainly limited to ablation through high intensity focused ultrasound (HIFU), but interesting preliminary results show that low frequency low intensity ultrasound (LILFU) could be instead used to modulate neural activity. However, the extent of this modulatory ability of US is still unclear, as in in vivo studies it is hard to disentangle the contribution to neural responses of direct activation of the neuron by US stimulation and indirect activation due either to sensory response to mechanical stimulation associated to US, or to propagation of activity from neighboring areas. Here, we aim at showing how to separate the three effects and assess the presence of direct response to US stimulation in zebrafish. *Approach:* We observed in zebrafish larvae brain-wide US-induced activity patterns through calcium imaging microscopy. Sensory response to mechanical stimulation was assessed with a US shield. Activity propagation was assessed with inter-area latency evaluation. *Main results*: We prove that in selected brain regions zebrafish neural response is mainly due to direct activation, later spreading to the other regions. Shielding the neurons from direct US stimulation resulted in a significantly attenuated response, showing that sensory stimulation does not play a prominent role. *Significance:* US non-invasive neuromodulatory approach might lead to novel ways to test and control neural activity, and hence to novel neuromodulatory therapies. Future studies will focus on the biophysical structure of directly responsive neurons to capture the mechanisms of US induced activity.

Keywords: neuromodulation, zebrafish, ultrasounds, calcium imaging

1. Introduction

The use of low intensity low frequency ultrasound (LILFU) to non-invasively modulate neuronal activity has been the focus of intense interest in the neural engineering communities over the last decade [1,2]. Studies have been performed investigating ultrasound (US) stimulation both in the peripheral [3–6] and specially in the central nervous system (CNS). In the CNS many animal models have been adopted

for such investigations: human [7–10] and non-human [11–13] primates, pigs [14,15], sheep [16], cats [17,18], lagomorphs [19], guinea pigs [20], rats [21–26], and mice [27–31].

A crucial open issue in US neuromodulation studies is to which extent observed responses are due to direct effects of US on neuronal channels [32] and membranes [33,34], rather than mechanical stimulation of sensory pathways propagating to other areas [20,28]. Current literature, however, lacks a thorough study on direct cortex-wide neuronal responses to US stimulation, able to map such propagation. Many works in this field have indeed adopted intracranial electrical recordings [14,15,20,31,35–37] that are logistically limited in the number of neurons, hence central nervous system (CNS) regions that can be simultaneously monitored. Fewer works have instead selected metabolic or hemodynamic acquisition paradigms (first and foremost PET and fMRI) [11,12,19,38–40] that, despite having the potential of recording the whole brain activity, only indirectly access neurons' activity. Recently, the use of transgenic zebrafish larvae pan-neuronally expressing the calcium indicator GCaMP6s [41], coupled with wide-field fluorescence imaging, has proven an effective means to non-invasively investigate neuronal activity. This experimental choice can indeed directly access brain-wide CNS activity patterns with relatively high spatiotemporal resolution [42].

Here we report the US-evoked activity patterns of larval zebrafish' encephalon gathered through wide-field calcium imaging microscopy. We devised an experimental paradigm enabling to carefully study the activity propagation across multiple brain areas and to discriminate mechanical sensory stimulation from direct activation.

2. Methods

2.1 Sample preparation

The analysis was performed on zebrafish larvae at three different (3,4 and 5) days post-fertilization (dpf). Unless otherwise stated all results refer to 5 dpf larvae. Adult and larval zebrafish were maintained for breeding at 28 °C on a 14/10 hours light/dark cycle according to standard procedure [43]. Larvae were raised up to 5 dpf in fish water (150 mg/L Instant Ocean, 6.9 mg/L NaH_2PO_4, 12.5 mg/L Na_2HPO_4, pH 7.2) in a Petri dish kept at 28 °C. We used 3 to 5 dpf transgenic Tg(elavl3:GCaMP6s) zebrafish larvae [44,45] in homozygous *albino* background to avoid the presence of skin pigments. Following [45], each larva was then transferred into an Eppendorf tube, containing in 1.5% w/v low gelling temperature agarose (A9414, Sigma) dissolved in fish water kept at 38 °C, and introduced into a glass capillary tube (O.D. 1.5mm) with a pipette. After gel polymerization, the larva was extruded from the capillary, laid in the center of the bottom of a small modified Petri dish (5 cm diameter with the central part of 2 cm diameter replaced by a 25 μm thin polystyrene membrane (Goodfellow, Hungtinton, Cambridge, UK)) and this position was blocked with a drop of melted agarose. After solidification the dish was filled with fish water. Fish rising and experiments were carried in accordance with European and Italian law on animal experimentation (D.L. 4 March 2014, n.26), under authorization n. 407/2015-PR from the Italian Ministry of Health.

2.2 US stimulation setup and transducer

US stimulation was applied by placing a 44 mm diameter PZT (Lead Zirconate Titanate) unfocused transducer (Precision Acoustics LTD, Dorchester, UK, S/N PA886, central frequency equal to 490 kHz, -3 dB bandwidth equal to 160 kHz, -6 dB X-profile beamwidth 19.88 mm, -6 dB Y-profile beamwidth 18.66 mm) at a distance of 165 mm from the animal specimen. The transducer was driven by a waveform generator (Agilent33220A Keysight Technologies, Santa Rosa, CA, USA) in series with a 50 dB gain radio frequency power amplifier (240L, Electronics & Innovation, Rochester, NY, USA) and it was immersed in the polymethyl methacrylate (PMMA) tank. The US transducer was characterized in free field conditions both in terms of ultrasonic pressure field mapping and intensity vs. driven voltage calibration. The pressure signals were detected by a 2 mm PVDF (Polyvinylidene Fluoride) needle hydrophone (Precision Acoustics LTD, Dorchester, UK, model number: NH2000) at different locations, using a three-axis step-by-step motorized positioning frame (XYZ BiSlide, Velmex, Bloomfield, NY, USA), thereby producing maps that provide information on the geometry of the generated acoustic field. A dedicated LabVIEW program (National Instruments, Austin, TX, USA) allowed synchronization between the wave generator, motors and signal acquisition from an oscilloscope (7034 B, InfiniiVision, Agilent Technologies). The root mean square pressure (P_{rms}) and the spatial peak pulse average intensity ($I_{sppa} = P_{rms}^2/(\rho\, c)$) were evaluated at the experimental distance of 165 mm at different driving voltages, each measured at the output of the power amplifier. The medium density $\rho = 1000\ Kg/m^3$ and the wave speed $c = 1484\ m/s$ are approximated to the density and speed of sound of water, respectively. The spatial peak temporal average intensity (I_{spta}) was defined as

$$I_{spta} = I_{sppa} * DC = \frac{P_{rms}^2}{\rho c} * DC \qquad (1)$$

where *DC* is the duty cycle used in the stimulation protocol. Finally, in order to consider possible acoustic reflections and attenuations phenomena, additional intensity measurements were performed by positioning the hydrophone tip inside the Petri dish used during experiments (see Figure S3 of [46] for

the results of the hydrophone measurements). These measurements yielded the I_{spta} calibration reported in Figure 1.

2.3 Stimulation protocol

Pulsed ultrasound stimulations of 490 kHz were delivered in blocks of three stimuli of 100 ms each, with a duty cycle of 25, 50, 75 or 100%. A stimulus duration of 300 ms with a pulse repetition frequency of 10 Hz was chosen. Pressure amplitude varied from 8 to 40 kPa in nine discrete steps. The I_{spta}, therefore, varied from 1.5 to 120 mW/cm^2. Each recording session consisted of three identical US stimulation windows delivered every 15 s. The overall acquisition time for every recording session was fixed at 60 s. We tested 12 3-dpf, 10 4-dpf, and 8 5-dpf larvae. Each larva has undergone two sets of nine recording sessions, one for each pressure amplitude. For each pressure amplitude, the duty cycle was first set at either 25% or 50% and then increased to 100% or 75%.

Following the results of a previous work of our group [46], we analysed the responses as function of the US spatial-peak temporal-average intensity I_{spta}, (see Eq.1 in section 2.2). To facilitate reading, we divided the stimulation acoustic intensity (I_{spta}, measured in mW/cm^2) into 5 balanced groups ranging from very low to very high (Figure 1c).

2.4 Imaging setup

Imaging of the agarose restrained larvae was performed using a custom-made upright fluorescence microscope in epi configuration. Fluorescence was excited in wide-field approach using an LED with emission centered at 470 nm (M470L3, Thorlabs), followed by a tube lens of 200 mm focal length (AC508-200-A, Thorlabs) and by an excitation band-pass filter (FF01-469/35 nm, Semrock). The fluorescence signal was collected by an air objective (Nikon, 10x, NA 0.3, WD 16 mm). The detection path was implemented with a dichroic mirror (DC FF495-DI02, Semrock), an emission band-pass filter (FF03-525/50nm, Semrock) and a tube lens of 200 mm focal length (AC508-200-A, Thorlabs) that created an image on a sCMOS camera (OrcaFlash 4.0 v3, Hamamatsu Photonics) with 16-bit dynamic range at a frame rate of 20 Hz.

2.4.1 X-Y drifts correction of calcium imaging videos.

Due to US-induced fish water movements, our measurements were affected by x-y and z drifts, producing both in-plane and out-of-focus artifacts, respectively. To correct for these artifacts, we used an open access algorithm programmed in Java and compatible with ImageJ, namely *moco* [47]. This choice was due to its accuracy (that is comparable to that of established community-used algorithms), its speed and its large stability to large translational motions (fundamental for our calcium imaging videos). Briefly, *moco* corrects every image in the video by comparing every possible translated version of it with a template image. In our case, the template was set to be the first frame of the video. The algorithm then identifies the translation term that minimizes the L_2 norm of the difference between the images in the overlapping region, D, divided by the area of D. As output, besides the corrected video frames, the algorithm provides for each image the amount of adjustment, in pixels, applied to correct for the in-plane x-y drifts, computed as the root mean square of the translation in the x and the y direction. This metric was used as an indirect measure of the water movements caused by the US stimulation.

2.5 Experimental design

2.5.1 US shielded experiments. In the experimental set-up larvae are placed in a Petri dish containing water (Figure 1). US stimulation induced waves in the water. On one hand the observed response could therefore be due to direct stimulation on ionic channels [32] and/or on neuronal membranes [33,34]. On the other hand, however, the recorded activation could be the consequence of the animal sensitivity to the US-induced water movements and/or to a vestibular stimulation [48]. Furthermore, the envelope of the three pulses composing each US stimulation window can be assimilated to a sound source centered at 10 Hz, although the auditory response of larval zebrafish in this low range is expected to present a much lower sensitivity than above 50 Hz [49]. To verify whether the induced neuronal activity was attributable to a direct US neuromodulation effect or to US-induced sensory stimulation, we performed control experiments, referred to as US-shielded. We placed in the path between the US transducer and the Petri dish a 10 mm thick soundproofing rectangular element. We used a blue polyurethane sheet (AptFlex F28, Precision Acoustics) with density and wave speed similar to that of water, but with significant absorption (acoustic impedance equal to 1.5 MRayls; insertion loss equal to 16 dB resulting in the transmission of the 15.85% of the incident acoustic pressure). This protocol allowed us to image larval CNS fluorescence dynamics without the brain being directly hit by the US, but while still making the surrounding watery media moving due to the sound stimulation waves.

The set of stimulations applied was the same as in the unshielded case. However, as the presence of the soundproofing element decreased the magnitude of water movements in the control experiments, compared to US-unshielded case, rather than comparing responses to the same stimulation, we compared four selected pressure level pairs that lead to similar amplitude of water movements for the two groups, as observed indirectly from the applied motion adjustment to the fluorescence images (see 2.4.1). In this way, we ensured that the difference in the response was solely due to direct activation. For example, we compared the post-stimulus $\Delta F/F_0$ of the US-shielded group at P_{RMS}=40 kPa with the ones of the US-unshielded experiments at P_{RMS}=28 kPa. Specifically, in Figure 3 the P_{RMS} corresponding to the water movement labels are: low: 16 kPa for US-unshielded and 24

kPa for US-shielded ; moderate: 20 kPa for US-unshielded and 28 kPa for US-shielded; considerate: 24 kPa for US-unshielded and 36 kPa for US-shielded; high: 28 kPa for US-unshielded and 40 kPa for US-shielded. Table 1 lists the estimated amplitude of water movements corresponding to the aforementioned US pressure amplitudes for both the experimental paradigms. The US-shielded group is made up of 8 3-dpf, 8 4-dpf, and 6 5-dpf larvae.

P_{RMS} for US-unshielded experiments	P_{RMS} for US-shielded experiments	Maximal US-induced water movements	Figure 3c water movement labels
16 kPa	24 kPa	19.2 µm	low
20 kPa	28 kPa	29.6 µm	moderate
24 kPa	36 kPa	43.2 µm	considerable
28 kPa	40 kPa	54.4 µm	high

Table 1: Estimated amplitude of US-induced water movements in the US-shielded and US-unshielded experiments.

2.6 Data analysis

2.6.1 Relative fluorescence variation. As common practice in calcium imaging video analysis, the fluorescence dynamics was expressed as:

$$\frac{\Delta F}{F_0}(t) = \frac{F(t) - F_0(t)}{F_0(t)} \quad (2)$$

where F(t) is the fluorescence intensity and $F_0(t)$ is the baseline fluorescence intensity at a given time instant t. To compute the baseline fluorescence, we used a running-window average of the 8th percentile of the fluorescence intensity F(t) [50]. We used a time window of 5 seconds, approximately 25 times larger than the decay time constant of the adopted calcium reporter [51]. $(\Delta F/F_0)_{max}$ was defined as the difference between the maximal value of $\Delta F/F_0$ traces following US stimulation and the $\Delta F/F_0$ value at stimulation onset.

Significant statistical differences in this value are assessed with Kruskal-Wallis test (p=0.05) and multiple comparison have been accounted for by the Dunn approach. The dependence of the response by multiple factors and their interaction was assessed by two-way analysis of variance (ANOVA) [52]. The same analysis was performed for the latency of the response (i.e., the time from US stimulus onset to maximal amplitude of $\Delta F/F_0$).

2.6.2 Spots of maximal and minimal activation. We identified, separately for every recording, the spots of maximal and minimal activation in the zebrafish encephalon following US stimulation considering the pixels (1.6×1.6 µm^2) whose summed fluorescence variation $\Delta F/F_0$ after the stimulus trigger was greater/lower than the 99-/1- percentile of the global relative fluorescence. The global relative fluorescence was defined as:

$$\left(\frac{\Delta F}{F_0}(t)\right)_{global} = \sum_{k=1}^{3} \sum_{t=t_k^*}^{t_k^*+5s} \frac{\Delta F}{F_0}(t) \quad (3)$$

where k is the US stimulus number (every recording consisted in three US stimuli), t_k^* is the corresponding US stimulus trigger instant and $\frac{\Delta F}{F_0}(t)$ is the relative fluorescence variation. After an imaging registration onto a common brain orientation step employing a roto-translation transformation, the binary maps of the spots obtained for different larvae with the same US intensity I_{spta} were summed and normalized to compute the spatial probability maps.

3. Results

US stimulations were tested on non-pigmented larval stages of zebrafish which ensured optimal visibility of calcium imaging response. All larvae belonged to a transgenic line expressing GCaMP6s [42] in all CNS neurons in order to visualize whole-CNS response. We devised a setup (Figure 1a) able to perform wide-field calcium imaging during simultaneous whole-brain stimulation through an ultrasound planar transducer.

3.1 Neural sensitivity to ultrasound stimulation is region-dependent

We observed simultaneously the response to US stimulation, measured as fluorescence variation (see Methods), in four well characterized regions of the CNS (Figure 2a). Both region and intensity played a significant role in determining the response (two-way ANOVA, $p<0.001$ for each factor, $p<0.001$ for their interaction). The cerebellum displayed the strongest response ($(\Delta F/F_0)_{max}$=7.1% for very high stimulation, Figure 2b bottom left) and the highest sensitivity to ultrasound stimulation, with significant differences between the response to most stimulus levels (Figure S1). The optic tectum and the medulla displayed a lesser response ($(\Delta F/F_0)_{max}$=5.8% and 5.45% respectively for very high stimulation, Figure 2b top and bottom right). The telencephalon displayed the weakest response ($(\Delta F/F_0)_{max}$=2.1% for very high stimulation, Figure 2b top left) with significant differences only between high/very high and low/very low intensity (Figure S1). We also identified for each stimulation pattern the spots of maximal and minimal

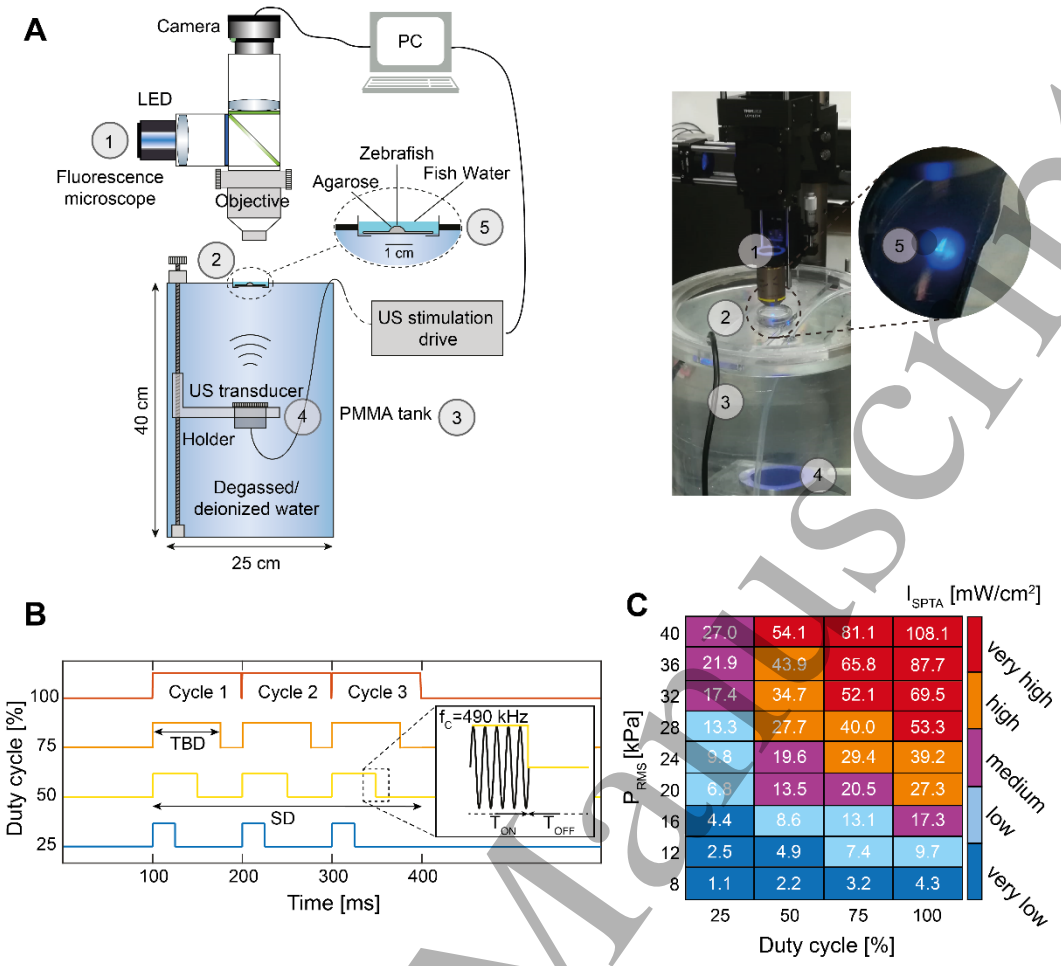

Figure 1: Experimental setup and stimulation parameters. (a) Illustrative scheme (left) and photo (right) of the experimental setup composed of a PMMA tank full of degassed deionized water (3) in which the 44 mm diameter PZT unfocused US transducer was immersed (4). On top of the tank a custom-made interlocking housing (2) contained a Petri dish filled with fish water in which the zebrafish larvae were immobilized with agarose (5). Above the setup, a custom-made upright fluorescence microscope in epi configuration (1) was used for imaging the encephalon of the mounted larvae. Each recording sessions lasted for 60 seconds during which 3 stimulations were triggered every 15 seconds by a waveform generator in series with a 50 dB gain radio frequency power amplifier. (b) Temporal protocol of US stimulation: duty cycle (DC) 25% (blue) with T_{ON}=25 ms and T_{OFF}=75 ms; DC 50% (yellow) with T_{ON} =50 ms and T_{OFF}=50 ms; DC 75% (orange) with T_{ON}=75 ms and T_{OFF}=25 ms; DC 100% (red) with T_{ON}=100 ms. The tone burst duration (TBD) is equal to T_{ON} and the pulse repetition period (PRP) is equal to 100 ms; the stimulation duration (SD) is of 300 ms for the four chosen temporal protocols. Each stimulation was repeated three times during every recording session with an inter stimulation interval of 15 s. In the inset it is shown the temporal evolution of US stimulation waves produced by a transducer with central frequency equal to 490 kHz. (c) Stimulation acoustic intensity (spatial peak temporal average measured in mW/cm^2) for each experimental protocol divided into 5 balanced groups. The set of used US intensities is within the range suggested by the FDA for diagnostic US imaging.

activation. Briefly, we defined as spots of maximal (minimal) activation those calcium imaging video pixels whose fluorescence variation after stimulus trigger was greater (lower) than the 99- (1-) percentile of global relative fluorescence (see Methods for details). Coherently with previous results, maximal and minimal activation spots were located for all animals in the cerebellum and in the telencephalon, respectively.

3.2 Comparing responses between unshielded and shielded US stimulation

Animals were positioned in a Petri dish filled with fish water during imaging. The US stimulation produced non negligible movements in such media. Consequently, the observed response could be due to a combination of direct stimulation on the ionic channels [32], on the neuronal membranes [33,34] and/or of the animal sensitivity to the US-induced water movements and sound perturbation at few Hz.

To elucidate how the calcium fluorescence activity patterns induced by the sonication could be accounted for by these two factors, we performed then US-shielded control experiments (see Methods) in which the larval brain was not directly hit by the US, but the surrounding watery media moved due to the incoming stimulation sound waves. We used the same set of US stimulations used in the unshielded animals and then we compared responses associated to the same level of sensory stimulation (see Methods). This allowed to estimate the response due to neuronal activation, while removing the contribution of sensory stimulation.

Responses to US stimulation were found to be much weaker in the US-shielded experiments as compared to the US-unshielded scenario and were elicited for a shorter time by a narrower set of stimulations (compare Figure 3a and 3b). In both experimental conditions, however, the cerebellum was the most responsive area, and we therefore compared the maximal amplitude of the two responses for the same levels of water movement (see Methods). We found that for all levels the response was significantly stronger in the unshielded condition ($p<0.01$) with an average of +199±94% (mean ± standard deviation) relative increase with respect to the shielded condition (Figure 3c).

3.3 Relative latency of US responses

We analysed then the temporal evolution of the response over the whole CNS in the US-unshielded experiments. We observed qualitatively that the first response in every I_{spta} group arose close to the maximal activation spot within the cerebellum, to later spread to other areas while increasing in intensity within the cerebellum (Figure 3a and Supp. Movie 1). We hypothesized then that at least for low stimulation intensities only these spots are activated by US stimulation, and all other responses are due to propagation of the activity. To test quantitatively this hypothesis, we calculated the latency of the response (i.e., the time from US stimulus onset to maximal amplitude of $\Delta F/F_0$) in each region, observing that it depended on both intensity and region ($p<<0.001$, two-way

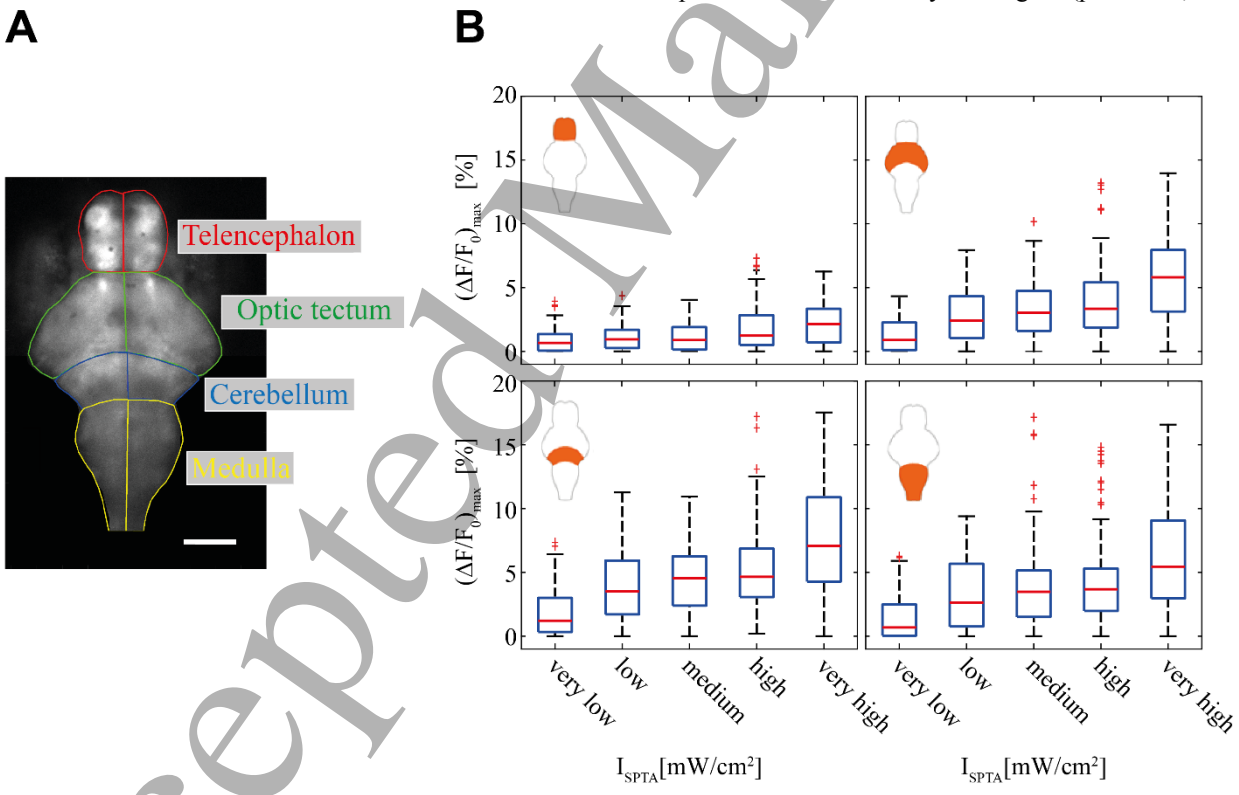

Figure 2: Neural sensitivity to ultrasound stimulation across regions (a) Wide-field fluorescence image of the encephalon of a representative larva expressing GCaMP6s. Scale bar: 100 µm. The four principal zebrafish brain regions used here for the analysis are highlighted (Telencephalon, red; Optic tectum, green; Cerebellum, blue; Medulla, yellow). (b) Boxplots of $(\Delta F/F_0)_{max}$ amplitude as a function of I_{spta} (divided into 5 groups) of four encephalon regions (schematically represented within the insets) for 5 dpf zebrafish larvae. Top left: Telencephalon; Top right: Optic tectum. Bottom left: Cerebellum; Bottom right: Medulla.

ANOVA), but not on their interaction (p=0.13, two-way ANOVA). We found that the spots of maximal activation were triggered significantly before all the other regions at very low intensity (Figure 4a top left and S2). This suggests that activity in all other regions at least for this intensity is not directly elicited by US, but by inputs from cerebellar afferences. The latency for the maximal activation spots did not depend on the intensity of the stimulation and was on average 1.5 s (Figure 4b). For the other areas the latency varied with the stimulation intensity. For higher intensities cerebellum, optic tectum and medulla displayed latencies closer to the one at the maximal activation spots (Figure 4a, 4c, and S2), which is compatible with direct US activation at these intensities. The telencephalon, instead, displayed an average latency which was always significantly higher than that of the other areas (Figure S2) and reached a minimum value of 3.7 s for the highest stimulation intensity (Figure 4a bottom right). In particular, the region of minimal activation within the telencephalon showed for all intensities a low-amplitude response starting more than one second after the end of US stimulation (Figure S3). This strongly suggest that the telencephalon is not activated directly by the US stimulation, but only by the propagation of activity from other areas (Figure 4c).

3.4 Evolution of US response with development

All results in the previous sections refer to 5 dpf larvae. As both single neuron properties and connectivity are expected to change during development [53,54], progressively expanding the larval cognitive and processing skills, we probed whether the sensitivity to US was present since the first tested larval stage and if it showed an increasing trend along dpf. To this end, we performed a finer analysis of the spots of maximal and minimal activation across the three tested days post fertilization.

The spots of minimal activation were confined to the larval telencephalon for every applied stimulus parameter and animal development stage (Fig 5a, right columns). The location of the spots of maximal activation (see Methods) confirmed instead that the strongest sensitivity to the US was confined to the cerebellum for every dpf (Figure 5a, left columns). More precisely, maximal activation was stereotypically (across animals and recordings) located near the border between the cerebellum and the upper portion of the medulla. Of note, the sensitivity to US of these subregions grew with the dpf (Figure 5b), confirming our expectation.

4. Discussion

4.1 Direct neural response vs sensory activation

The main aim of this work was to observe, isolate and characterize a direct neural response to US stimulation. By comparing neural responses in US-unshielded and US-shielded conditions, we were able to evaluate the extent of sensory contribution to such responses, and hence highlight the prominent role of direct response to US stimulation (Figure 3). The entanglement between direct and sensory mediated neural response to US stimulation has been debated in several recent works, examining, in particular, the neuromodulation activity triggered by transcranial US brain stimulation. Wide-field calcium imaging of transgenic mice brains was used to observe the neuronal activation due to US stimulation on the visual cortex, at a central frequency of 500 kHz [55]. While the US focus was on the visual area, the first strong activation was observed on the auditory cortex, starting from the contralateral hemisphere, with a response similar to the one elicited by audible sounds. The excitation effect increased with the stimulation intensity in this region, but the activation spread onto a larger cortical area. This suggested that the observed neural activation was due to acoustic stimulation of the inner ear, rather than direct neural activation. Moreover, the response to both US and sound was attenuated in chemically deafened animals and disappeared when the transducer was not coupled to the head.

The companion study [20] investigated the effect of 220 kHz US stimulation on guinea pig brain, recording local field potentials (LFPs) from auditory cortex and inferior colliculus. Responses occurred whenever the transducer was in contact with the animal head or the eyeball. However, the first spike latency was shorter in the inferior colliculus, suggesting that the recorded signal in the auditory cortex should be the consequence of sensory stimulation. The response of the somatosensory cortex was largely independent from the transducer focus, suggesting that motor cortex elicitation might be caused by startle reflex. This US-induced cortical activation was completely abolished by auditory nerve transection and removal of cochlear fluids. Such results are in contrast with other works reporting the activation of a functional circuit associated to tactile sensation due to US stimulation in the somatosensory area [8,12]. Moreover, other studies have found a significant effect of the ultrasound stimulation target location [56,57].

These results are far from being conclusive. A work focusing on confounding activation of auditory pathways [58] observed auditory brainstem response that elicited EMG in forelimbs triceps in transgenic deaf mice. Another recent work observed US response in deep brain areas of macaques and their propagation to other brain regions [59]. They ruled out auditory stimulation confounding by an analysis of the correlation of such responses with auditory cortex activity. For zebrafish larvae there was no possible direct auditory confounding as the animal at this stage is not sensitive to such high frequency [60]. Nevertheless, auditory stimulation within its hearing range [61] may be produced by the pulsed stimulation sequence envelope that can be assimilated to a

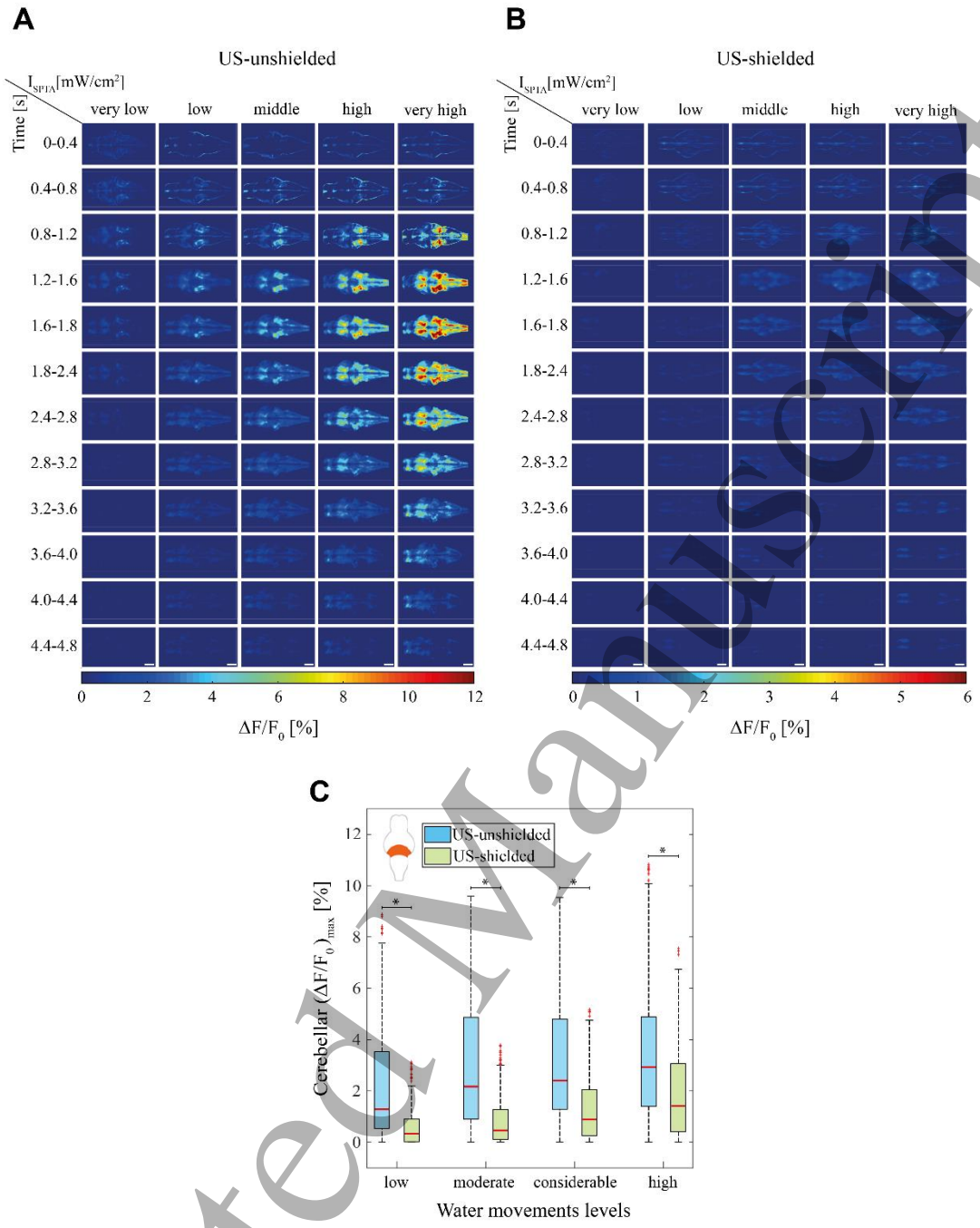

Figure 3. Comparison between responses in US-unshielded and US-shielded condition. (a) Mean pixel-wise $\Delta F/F_0$ maps following US stimulation for 5 dpf larvae, binned in 400 ms time windows, of the five I_{SPTA} families for the US-unshielded (i.e., without the soundproofing element) experiments. White bar in bottom row indicates 100 µm scale. (b) Same as (a), but for US-shielded experiments. (c) US-unshielded (light blue) and US-shielded experiments (green) comparison at equal magnitude of water movement. The boxplot depicts the distribution of cerebellar $\Delta F/F_0$ amplitude. The inset schematically represents the cerebellum within the zebrafish encephalon. Statistically significant differences are represented through asterisks (Wilcoxon's rank-sum test adjusted with Bonferroni correction, hence $p<0.01$).

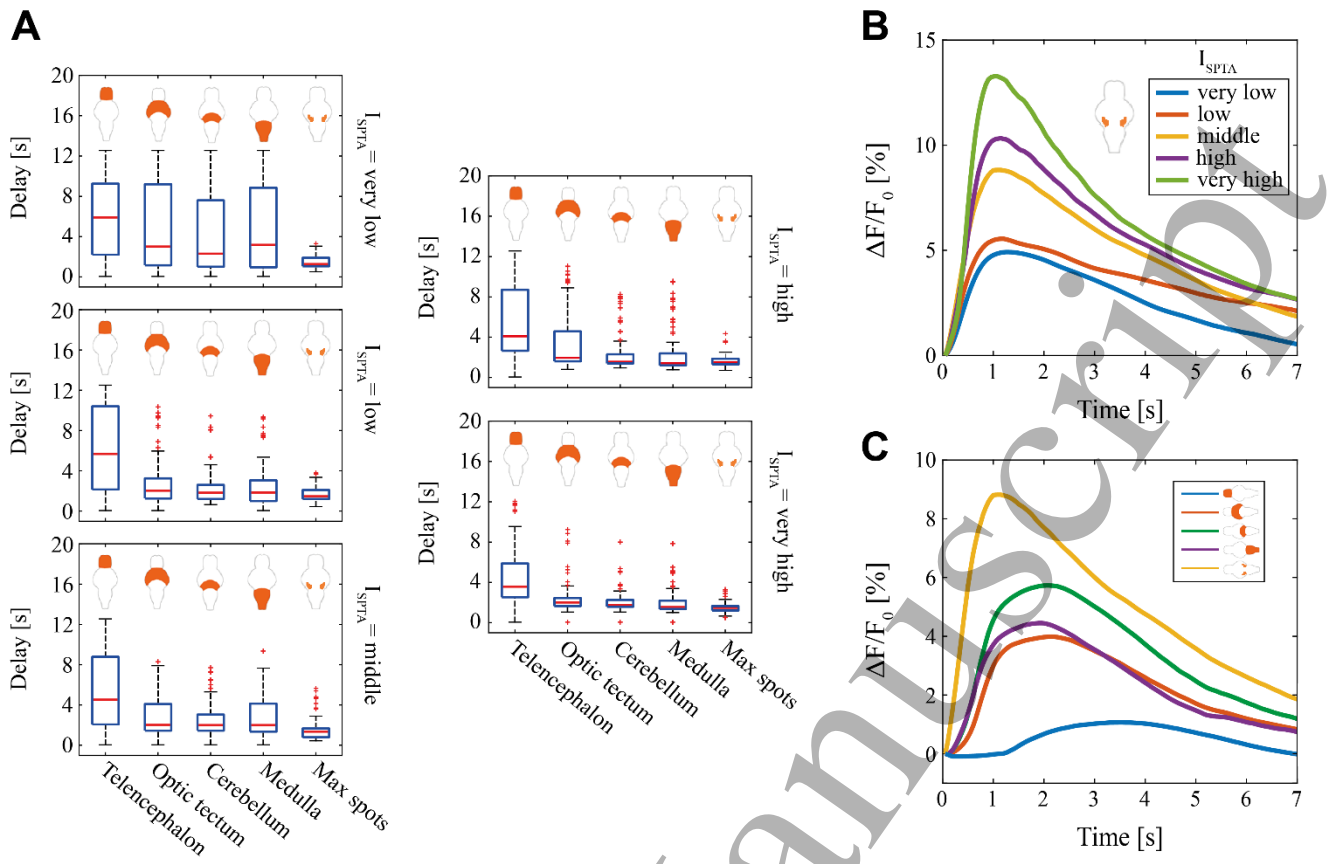

Figure 4. Temporal evolution of response to US stimulation. (a) Response latency in the 4 regions and in the spots of maximal activation in 5 dpf larvae for the five applied families of stimulation intensity I_{spta}. The inset schematically represents the region position in the zebrafish encephalon. (b) Fluorescence variation $\Delta F/F_0$ of the spots of maximal activation as a function of I_{spta}. (c) Fluorescence variation $\Delta F/F_0$ between encephalic areas for middle I_{spta}.

weak noisy sound source centered at 10 Hz. A recent hearing assessment study in larval zebrafish [49] has found that 20 Hz frequencies can be perceived with an approximately hundred times lower sensitivity than above 50 Hz. Consequently, we cannot exclude that zebrafish larvae are able to perceive sound even below 20 Hz, but with a further reduced sensitivity. Furthermore, we still had to investigate the possibility of mechanosensory confounding to tactile perception of US-induced waves in the water (Figure 3a). Moreover, despite our efforts into immobilizing the animals during recording, we could not discard the possible contribution of a vestibular response in the unshielded experiments [48]. Responses due to mechanical (and possibly vestibular and auditory) stimulation in the US-shielded condition were found to be significantly smaller than those induced in the US-unshielded case for all intensities (Figure 3b).

4.2 Area specificity

We have shown selective activation of zebrafish brain areas. Such a selectivity is not a complete novelty: for instance, in their seminal work [19] Yoo and colleagues observed that the US stimulation effect was stronger in motor than in visual cortex. In a more recent work [62], the mice awake cortex was stimulated while monitoring the hemodynamic change of the whole cortex due to the different stimulation protocols and observed local responses. However, to the best of our knowledge, our study is the first to exploit the simultaneous monitoring of the whole CNS to discriminate between direct, primary activation and secondary activation. In a much narrower context, propagation of US response was observed in experiments with stimulation of primary somatosensory cortex on monkeys [12]. It was indeed found that US stimulation not only activated the cortical area corresponding to the focus, but also spatially distant regions corresponding to the touch processing circuitry. The observed increase in response strength with dpf is consistent with the progressive development of the larval CNS with age.

4.3 Inter-area propagation of the response

The aim of our analysis of temporal evolution was to assess whether neurons in different regions were activated directly by US stimulation or were rather triggered by functionally connected regions. We noted that, as a consequence of US stimulation, the cerebellar area was the first one to respond.

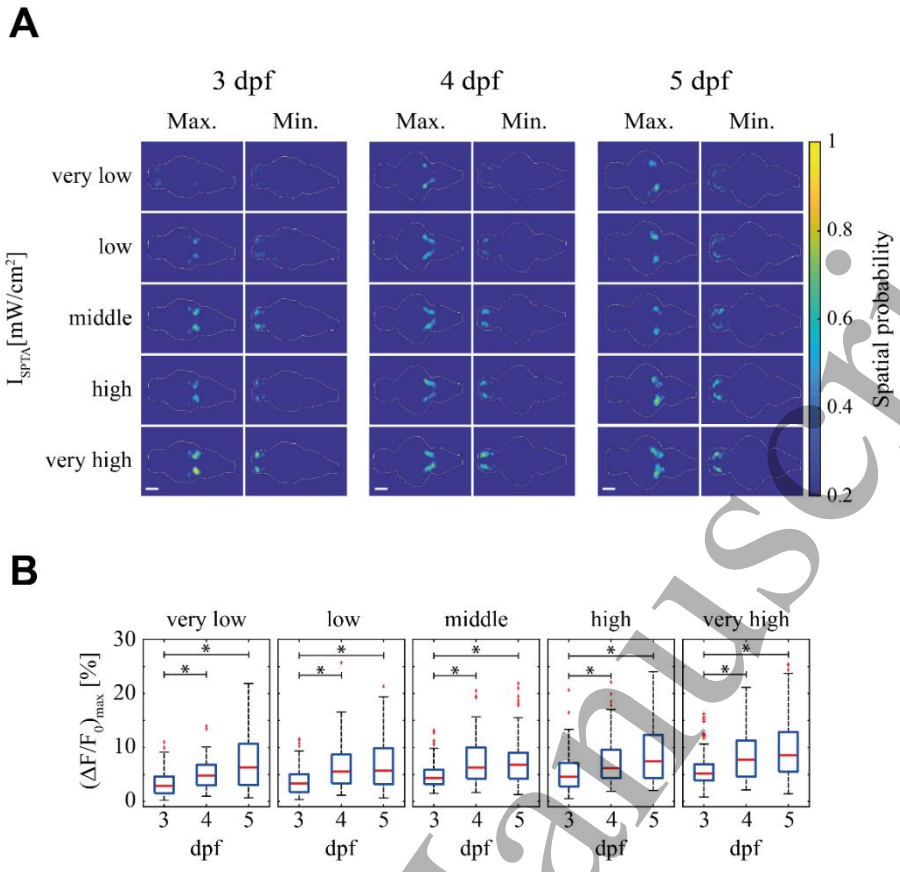

Figure 5. Evolution of response to US stimulation with zebrafish development. (a) Spatial probability distribution of the spots of maximal (> 99% overall response, left columns) and minimal activation (<1% overall response, right columns) as a function of the five I_{spta} families for each tested day post fertilization. (b) Boxplots of maximal fluorescence variation amplitude $(\Delta F/F_0)_{max}$ as a function of the days post fertilization for the five I_{spta} families. Asterisks indicate significant statistical differences.

Right after cerebellar response, we observed a consistent activation of striped nuclei spanning the entire medulla down to the spinal cord (see Figure 3a, 4, S2 and Supp. Movie 1), presumably signs of functional connection with a motor circuit. The telencephalon was the last activated area and showed a response so late (Figure S3) to be consistent with an activity exclusively due to the propagation of the response induced by US in other areas of the CNS (Figure 4c). Crucially, our work aims at discriminating between primary and secondary activation looking at the relative times of activation of the different areas rather than determining the absolute latency of the response, which is difficult to assess given the inherently slow dynamics of calcium imaging responses [55]. Indeed the latencies reported here are one order of magnitude larger than the ones previously reported for cellular response [46] or even motor activity following stimulation [31,63] .

4.4 Thermal effect of US

US are known to interact with biological tissues through either thermal or non-thermal physical mechanisms. US-induced heat generation is dependent on several factors that can be controlled through proper choice of the stimulation parameters. The main factors contributing to the conversion of ultrasonic energy to heat are [64]: (i) the tissue properties (most and foremost the absorption coefficients and the impedance mismatch encountered by the ultrasonic waves); (ii) the US exposure parameters (mainly the frequency, the pressure amplitude, the pulse repetition frequency, and the pulse duration); (iii) the beam configuration. Considering these three factors in our experiments, we can rule out the recorded responses to be ascribable to significant thermal effects.

A recent modeling study [65], revealed, through retrospective temperature simulation, that thermal effects can be neglected in a large set of rodent setups. Only in one study [66], it was estimated a temperature increase as high as 7°C due to thermal

diffusion from the skull bone into the brain tissue; this was mainly due to the skull absorption coefficient [65], which in rodents is ten times higher than the soft brain tissue (α=2.7 dB/cm/MHz$^{1.18}$ in the skull, α=0,21 dB/cm/MHz$^{1.18}$). In our experiments, however, skull-induced heating is not present as in zebrafish skull bones develop and ossify long after the embryonic period. At larval stages, indeed, the craniofacial skeleton is primarily composed of cartilage elements often one or a few cell layers thick [67].

Furthermore, we choose to place the US transducer in water in order to minimize the heat produced by the probe itself when it is operated in air [68] and to provide thermal stabilization and water coupling of the ultrasound probe to the Petri dish.

As for the US stimulation parameters employed in our study, many studies [64,69–72] have pointed out that US exposure protocols consisting of low pressures (< 0.6 MPa at focus), low frequencies (sub-MHz), short pulse durations (≤ 300 ms), and low acoustic intensities (in the 30–500 mW/cm^2 range) do not lead to thermal effects playing a prominent role in neuromodulation, with estimated temperature rise as low as hundredths of a degree. Additionally, we have adopted a pulsed exposure delivery mode of ultrasonic stimuli, that is known to further minimize the probability of tissue heating [38,64,73,74].

Finally, we choose to employ an unfocused US transducer to stimulate the whole zebrafish encephalon. The absence of a small focal area furtherly minimizes the energy concentration and consequent heat production in the zebrafish encephalon. Altogether these considerations can therefore rule out possible significant thermal effects in the fluorescence increase we recorded in the zebrafish encephalon.

4.5 Limitations

We found that specific areas within the zebrafish cerebellum are highly sensitive to direct US stimulation, as pointed out by the spatial and temporal comparison between the neural responses with US-unshielded and US-shielded stimulation. Still, within the adopted experimental paradigm, it is not possible to completely rule out that the observed response contains a sensory-mediated contribution, originated from mechanical water motion and possibly vestibular and auditory perception. The current knowledge of the properties of zebrafish neurons does not allow us to understand what are the specific characteristics of the cerebellum that make it markedly sensitive to US. A full understanding of the biophysical dynamics leading to direct activation goes indeed beyond the scope of this work. Understanding these dynamics would be of paramount importance for a proper design of the stimulation, and, even more important to assess the likelihood of the possibility to directly stimulate neurons also in other animals (see [46]) and in particular in humans for translational applications.

5. Conclusions

Using an unfocused planar transducer and an *ad hoc* setup we were able to deliver ultrasonic stimulation to larval zebrafish' CNS. We managed to induce a reliable neuronal response in the animals' encephalon.

Control experiments were conducted to disambiguate the US direct effects on the animals' CNS and the sensory perception of the stimulation-induced water movements and spurious low frequency acoustic noise. We proved that the analysed calcium fluorescence activity patterns are not solely caused by these confounding sources, hence highlighting a direct role played by US in increasing the probability of neural activation. The compound contribution of the US stimulation and the consequently induced water movements in the unshielded experiments was however inextricable with the experimental paradigm adopted here, and further efforts should, therefore, be made to completely disambiguate the role of water movements in the reported results.

The strongest and quickest response was found to be highly consistent across animals and confined in a cerebellar subregion. It was present in all tested dpf and grew in strength concurrently with the CNS development. The activation probability and the fluorescence variation of this region was observed to be positively modulated both by stimulus magnitude (i.e., pressure, P_{RMS}) and duration (i.e., duty cycle), in accordance with previous results in a different animal models [46]. The subsequent activation of neighboring CNS areas can be interpreted as due to their functional connection with a motor circuit. In the future, a finer identification of those functionally related nuclei and a better characterization of the spatial dynamics occurring during US stimulation will necessarily require a real-time whole-brain approach through microscopy techniques endowed with optical sectioning as light-sheet microscopy [75–81].

This regionality of the response suggests a dependence of this neuromodulation strategy on neuronal population characteristics and architecture. Further characterization of the relationship between single cells properties and sonication parameters could, therefore, shed clearer light on the basic mechanisms of US neuromodulation.

Acknowledgements

This work has received funding from the European Research Council (ERC) under grant agreement ID No. 692943 (BrainBIT) and from the Italian Ministry of Education, University and Research (MIUR) through PRIN-2017 "PROTECTION" (project 20178L7WRS) and in the framework of Eurobioimaging (ESFRI research infrastructure) - Advanced Light Microscopy Italian Node. It was also partially funded by the Swiss National Science Foundation via the National Competence Center Research (NCCR) Robotics and the Bertarelli Foundation.

References

[1] Landhuis E 2017 Ultrasound for the brain *Nature* **551** 257–9

[2] Tyler W J, Tufail Y, Finsterwald M, Tauchmann M L, Olson E J and Majestic C 2008 Remote excitation of neuronal circuits using low-intensity, low-frequency ultrasound *PLoS ONE* **3** e3511

[3] Ilham S J, Chen L, Guo T, Emadi S, Hoshino K and Feng B 2018 In vitro single-unit recordings reveal increased peripheral nerve conduction velocity by focused pulsed ultrasound *Biomed Phys Eng Express* **4**

[4] Kim H, Taghados S J, Fischer K, Maeng L-S, Park S and Yoo S-S 2012 Noninvasive Transcranial Stimulation of Rat Abducens Nerve by Focused Ultrasound *Ultrasound in Medicine & Biology* **38** 1568–75

[5] Wright C J, Rothwell J and Saffari N 2015 Ultrasonic stimulation of peripheral nervous tissue: an investigation into mechanisms *J. Phys.: Conf. Ser.* **581** 012003

[6] Wright C J, Haqshenas S R, Rothwell J and Saffari N 2017 Unmyelinated Peripheral Nerves Can Be Stimulated in Vitro Using Pulsed Ultrasound *Ultrasound in Medicine & Biology* **43** 2269–83

[7] Legon W, Bansal P, Tyshynsky R, Ai L and Mueller J K 2018 Transcranial focused ultrasound neuromodulation of the human primary motor cortex *Sci Rep* **8** 10007

[8] Lee W, Chung Y A, Jung Y, Song I-U and Yoo S-S 2016 Simultaneous acoustic stimulation of human primary and secondary somatosensory cortices using transcranial focused ultrasound *BMC Neurosci* **17** 68

[9] Hameroff S, Trakas M, Duffield C, Annabi E, Gerace M B, Boyle P, Lucas A, Amos Q, Buadu A and Badal J J 2013 Transcranial Ultrasound (TUS) Effects on Mental States: A Pilot Study *Brain Stimulation* **6** 409–15

[10] Monti M M, Schnakers C, Korb A S, Bystritsky A and Vespa P M 2016 Non-Invasive Ultrasonic Thalamic Stimulation in Disorders of Consciousness after Severe Brain Injury: A First-in-Man Report *Brain Stimulation* **9** 940–1

[11] Verhagen L, Gallea C, Folloni D, Constans C, Jensen D E, Ahnine H, Roumazeilles L, Santin M, Ahmed B, Lehericy S, Klein-Flügge M C, Krug K, Mars R B, Rushworth M F, Pouget P, Aubry J-F and Sallet J 2019 Offline impact of transcranial focused ultrasound on cortical activation in primates *eLife* **8** e40541

[12] Yang P-F, Phipps M A, Newton A T, Chaplin V, Gore J C, Caskey C F and Chen L M 2018 Neuromodulation of sensory networks in monkey brain by focused ultrasound with MRI guidance and detection *Sci Rep* **8** 7993

[13] Lin Z, Meng L, Zou J, Zhou W, Huang X, Xue S, Bian T, Yuan T, Niu L, Guo Y and Zheng H 2020 Non-invasive ultrasonic neuromodulation of neuronal excitability for treatment of epilepsy *Theranostics* **10** 5514–26

[14] Dallapiazza R F, Timbie K F, Holmberg S, Gatesman J, Lopes M B, Price R J, Miller G W and Elias W J 2018 Noninvasive neuromodulation and thalamic mapping with low-intensity focused ultrasound *Journal of Neurosurgery* **128** 875–84

[15] Daniels D, Sharabi S, Last D, Guez D, Salomon S, Zivli Z, Castel D, Volovick A, Grinfeld J, Rachmilevich I, Amar T, Liraz-Zaltsman S, Sargsyan N, Mardor Y and Harnof S 2018 Focused Ultrasound-Induced Suppression of Auditory Evoked Potentials in Vivo *Ultrasound in Medicine & Biology* **44** 1022–30

[16] Lee W, Lee S D, Park M Y, Foley L, Purcell-Estabrook E, Kim H, Fischer K, Maeng L-S and Yoo S-S 2016 Image-Guided Focused Ultrasound-Mediated Regional Brain Stimulation in Sheep *Ultrasound in Medicine & Biology* **42** 459–70

[17] Ballantine H T, Bell E and Manlapaz J 1960 Progress and Problems in the Neurological Applications of Focused Ultrasound *Journal of Neurosurgery* **17** 858–76

[18] Fry F J, Ades H W and Fry W J 1958 Production of Reversible Changes in the Central Nervous System by Ultrasound *Science* **127** 83–4

[19] Yoo S-S, Bystritsky A, Lee J-H, Zhang Y, Fischer K, Min B-K, McDannold N J, Pascual-Leone A and Jolesz F A 2011 Focused ultrasound modulates region-specific brain activity *NeuroImage* **56** 1267–75

[20] Guo H, Hamilton M, Offutt S J, Gloeckner C D, Li T, Kim Y, Legon W, Alford J K and Lim H H 2018 Ultrasound Produces Extensive Brain Activation via a Cochlear Pathway *Neuron* **98** 1020-1030.e4

[21] Kim H, Lee S D, Chiu A, Yoo S-S and Park S 2013 Estimation of the spatial profile of neuromodulation and the temporal latency in motor responses induced by focused ultrasound brain stimulation: *NeuroReport* 1

[22] Han S, Kim M, Kim H, Shin H and Youn I 2018 Ketamine Inhibits Ultrasound Stimulation-Induced Neuromodulation by Blocking Cortical Neuron Activity *Ultrasound in Medicine & Biology* **44** 635–46

[23] Gulick D W, Li T, Kleim J A and Towe B C 2017 Comparison of Electrical and Ultrasound Neurostimulation in Rat Motor Cortex *Ultrasound in Medicine & Biology* **43** 2824–33

[24] Darvas F, Mehić E, Caler C J, Ojemann J G and Mourad P D 2016 Toward Deep Brain Monitoring with Superficial EEG Sensors Plus Neuromodulatory Focused Ultrasound *Ultrasound in Medicine & Biology* **42** 1834–47

[25] Yu K, Sohrabpour A and He B 2016 Electrophysiological Source Imaging of Brain Networks Perturbed by Low-Intensity Transcranial Focused Ultrasound *IEEE Trans. Biomed. Eng.* **63** 1787–94

[26] Koroleva V I, Vykhodtseva N I and Elagin V A 1986 Cortical and subcortical spreading depression in rats

produced by focused ultrasound *Neurophysiology* **18** 43–8

[27] Fisher J A N and Gumenchuk I 2018 Low-intensity focused ultrasound alters the latency and spatial patterns of sensory-evoked cortical responses *in vivo J. Neural Eng.* **15** 035004

[28] Sato T, Shapiro M G and Tsao D Y 2018 Ultrasonic Neuromodulation Causes Widespread Cortical Activation via an Indirect Auditory Mechanism *Neuron* **98** 1031-1041.e5

[29] Li G-F, Zhao H-X, Zhou H, Yan F, Wang J-Y, Xu C-X, Wang C-Z, Niu L-L, Meng L, Wu S, Zhang H-L, Qiu W-B and Zheng H-R 2016 Improved Anatomical Specificity of Non-invasive Neuro-stimulation by High Frequency (5 MHz) Ultrasound *Sci Rep* **6** 24738

[30] Ye P P, Brown J R and Pauly K B 2016 Frequency Dependence of Ultrasound Neurostimulation in the Mouse Brain *Ultrasound in Medicine & Biology* **42** 1512–30

[31] Tufail Y, Matyushov A, Baldwin N, Tauchmann M L, Georges J, Yoshihiro A, Tillery S I H and Tyler W J 2010 Transcranial Pulsed Ultrasound Stimulates Intact Brain Circuits *Neuron* **66** 681–94

[32] Kubanek J, Shukla P, Das A, Baccus S A and Goodman M B 2018 Ultrasound Elicits Behavioral Responses through Mechanical Effects on Neurons and Ion Channels in a Simple Nervous System *J. Neurosci.* **38** 3081–91

[33] Plaksin M, Shapira E, Kimmel E and Shoham S 2018 Thermal Transients Excite Neurons through Universal Intramembrane Mechanoelectrical Effects *Phys. Rev. X* **8** 011043

[34] Lemaire T, Neufeld E, Kuster N and Micera S 2019 Understanding ultrasound neuromodulation using a computationally efficient and interpretable model of intramembrane cavitation *J. Neural Eng.* **16** 046007

[35] Choi J B, Lim S H, Cho K W, Kim D H, Jang D P and Kim I Y 2013 The effect of focused ultrasonic stimulation on the activity of hippocampal neurons in multi-channel electrode *2013 6th International IEEE/EMBS Conference on Neural Engineering (NER)* 2013 6th International IEEE/EMBS Conference on Neural Engineering (NER) (San Diego, CA, USA: IEEE) pp 731–4

[36] Wattiez N, Constans C, Deffieux T, Daye P M, Tanter M, Aubry J-F and Pouget P 2017 Transcranial ultrasonic stimulation modulates single-neuron discharge in macaques performing an antisaccade task *Brain Stimulation* **10** 1024–31

[37] Prieto M L, Firouzi K, Khuri-Yakub B T and Maduke M 2018 Activation of Piezo1 but Not NaV1.2 Channels by Ultrasound at 43 MHz *Ultrasound in Medicine & Biology* **44** 1217–32

[38] Legon W, Rowlands A, Opitz A, Sato T F and Tyler W J 2012 Pulsed Ultrasound Differentially Stimulates Somatosensory Circuits in Humans as Indicated by EEG and fMRI ed M Ptito *PLoS ONE* **7** e51177

[39] Lee W, Kim H-C, Jung Y, Chung Y A, Song I-U, Lee J-H and Yoo S-S 2016 Transcranial focused ultrasound stimulation of human primary visual cortex *Sci Rep* **6** 34026

[40] Ai L, Mueller J K, Grant A, Eryaman Y and Legon W 2016 Transcranial focused ultrasound for BOLD fMRI signal modulation in humans *2016 38th Annual International Conference of the IEEE Engineering in Medicine and Biology Society (EMBC)* 2016 38th Annual International Conference of the IEEE Engineering in Medicine and Biology Society (EMBC) (Orlando, FL, USA: IEEE) pp 1758–61

[41] Ahrens M B, Orger M B, Robson D N, Li J M and Keller P J 2013 Whole-brain functional imaging at cellular resolution using light-sheet microscopy *Nat Methods* **10** 413–20

[42] Turrini L, Fornetto C, Marchetto G, Müllenbroich M C, Tiso N, Vettori A, Resta F, Masi A, Mannaioni G, Pavone F S and Vanzi F 2017 Optical mapping of neuronal activity during seizures in zebrafish *Sci Rep* **7** 3025

[43] Westerfield M *The Zebrafish Book: A Guide for the Laboratory Use of Zebrafish* (Univ. of Oregon Press, Eugene)

[44] Ahrens M B, Orger M B, Robson D N, Li J M and Keller P J 2013 Whole-brain functional imaging at cellular resolution using light-sheet microscopy *Nat Methods* **10** 413–20

[45] Turrini L, Fornetto C, Marchetto G, Müllenbroich M C, Tiso N, Vettori A, Resta F, Masi A, Mannaioni G, Pavone F S and Vanzi F 2017 Optical mapping of neuronal activity during seizures in zebrafish *Sci Rep* **7** 3025

[46] Dedola F, Ulloa Severino F, Meneghetti N, Lemaire T, Cafarelli A, Ricotti L, Menciassi A, Cutrone A, Mazzoni A and Micera S 2020 Ultrasound stimulations induce prolonged depolarization and fast action potentials in leech neurons *IEEE Open J. Eng. Med. Biol.* 1–1

[47] Dubbs A, Guevara J and Yuste R 2016 moco: Fast Motion Correction for Calcium Imaging *Front. Neuroinform.* **10**

[48] Migault G, van der Plas T L, Trentesaux H, Panier T, Candelier R, Proville R, Englitz B, Debrégeas G and Bormuth V 2018 Whole-Brain Calcium Imaging during Physiological Vestibular Stimulation in Larval Zebrafish *Current Biology* **28** 3723-3735.e6

[49] Yao Q, DeSmidt A A, Tekin M, Liu X and Lu Z 2016 Hearing Assessment in Zebrafish During the First Week Postfertilization *Zebrafish* **13** 79–86

[50] Dombeck D A, Khabbaz A N, Collman F, Adelman T L and Tank D W 2007 Imaging Large-Scale Neural Activity with Cellular Resolution in Awake, Mobile Mice *Neuron* **56** 43–57

[51] Romano S A, Pérez-Schuster V, Jouary A, Boulanger-Weill J, Candeo A, Pietri T and Sumbre G 2017 An integrated calcium imaging processing toolbox for the

analysis of neuronal population dynamics ed L J Graham *PLoS Comput Biol* **13** e1005526

[52] Montgomery D C, Runger G C and Hubele N F 2011 *Engineering statistics* (Hoboken, NJ: John Wiley)

[53] Kimmel C B 1993 Patterning the Brain of the Zebrafish Embryo *Annu. Rev. Neurosci.* **16** 707–32

[54] Schmidt R, Strähle U and Scholpp S 2013 Neurogenesis in zebrafish – from embryo to adult *Neural Dev* **8** 3

[55] Sato T, Shapiro M G and Tsao D Y 2018 Ultrasonic Neuromodulation Causes Widespread Cortical Activation via an Indirect Auditory Mechanism *Neuron* **98** 1031-1041.e5

[56] Mueller J, Legon W, Opitz A, Sato T F and Tyler W J 2014 Transcranial Focused Ultrasound Modulates Intrinsic and Evoked EEG Dynamics *Brain Stimulation* **7** 900–8

[57] Deffieux T, Younan Y, Wattiez N, Tanter M, Pouget P and Aubry J-F 2013 Low-Intensity Focused Ultrasound Modulates Monkey Visuomotor Behavior *Current Biology* **23** 2430–3

[58] Mohammadjavadi M, Ye P P, Xia A, Brown J, Popelka G and Pauly K B 2019 Elimination of peripheral auditory pathway activation does not affect motor responses from ultrasound neuromodulation *Brain Stimulation* **12** 901–10

[59] Folloni D, Verhagen L, Mars R B, Fouragnan E, Constans C, Aubry J-F, Rushworth M F S and Sallet J 2019 Manipulation of Subcortical and Deep Cortical Activity in the Primate Brain Using Transcranial Focused Ultrasound Stimulation *Neuron* **101** 1109-1116.e5

[60] Monroe J D, Manning D P, Uribe P M, Bhandiwad A, Sisneros J A, Smith M E and Coffin A B 2016 Hearing sensitivity differs between zebrafish lines used in auditory research *Hearing Research* **341** 220–31

[61] Privat M, Romano S A, Pietri T, Jouary A, Boulanger-Weill J, Elbaz N, Duchemin A, Soares D and Sumbre G 2019 Sensorimotor Transformations in the Zebrafish Auditory System *Current Biology* **29** 4010-4023.e4

[62] Kim E, Anguluan E and Kim J G 2017 Monitoring cerebral hemodynamic change during transcranial ultrasound stimulation using optical intrinsic signal imaging *Sci Rep* **7** 13148

[63] Kim H-J, Jeon B S, Paek S H, Lee K-M, Kim J-Y, Lee J-Y, Kim H J, Yun J Y, Kim Y E, Yang H-J and Ehm G 2014 Long-term cognitive outcome of bilateral subthalamic deep brain stimulation in Parkinson's disease *J. Neurol.* **261** 1090–6

[64] Dalecki D 2004 Mechanical Bioeffects of Ultrasound *Annu. Rev. Biomed. Eng.* **6** 229–48

[65] Constans C, Mateo P, Tanter M and Aubry J-F 2018 Potential impact of thermal effects during ultrasonic neurostimulation: retrospective numerical estimation of temperature elevation in seven rodent setups *Phys. Med. Biol.* **63** 025003

[66] Kamimura H A S, Wang S, Chen H, Wang Q, Aurup C, Acosta C, Carneiro A A O and Konofagou E E 2016 Focused ultrasound neuromodulation of cortical and subcortical brain structures using 1.9 MHz: FUS neuromodulation of cortical/subcortical brain structures *Med. Phys.* **43** 5730–5

[67] Mork L and Crump G 2015 Zebrafish Craniofacial Development *Current Topics in Developmental Biology* vol 115 (Elsevier) pp 235–69

[68] Miller D L and Zhou W 2013 A System for Investigation of Biological Effects of Diagnostic Ultrasound on Development of Zebrafish Embryos *Zebrafish* **10** 459–65

[69] Blackmore J, Shrivastava S, Sallet J, Butler C R and Cleveland R O 2019 Ultrasound Neuromodulation: A Review of Results, Mechanisms and Safety *Ultrasound in Medicine & Biology* **45** 1509–36

[70] Naor O, Krupa S and Shoham S 2016 Ultrasonic neuromodulation *J. Neural Eng.* **13** 031003

[71] Tyler W J, Tufail Y, Finsterwald M, Tauchmann M L, Olson E J and Majestic C 2008 Remote Excitation of Neuronal Circuits Using Low-Intensity, Low-Frequency Ultrasound ed H Tanimoto *PLoS ONE* **3** e3511

[72] O'Brien Jr. W 2007 Ultrasound–biophysics mechanisms *Progress in Biophysics and Molecular Biology* **93** 212–55

[73] Fini M and Tyler W J 2017 Transcranial focused ultrasound: a new tool for non-invasive neuromodulation *International Review of Psychiatry* **29** 168–77

[74] Legon W, Sato T F, Opitz A, Mueller J, Barbour A, Williams A and Tyler W J 2014 Transcranial focused ultrasound modulates the activity of primary somatosensory cortex in humans *Nat Neurosci* **17** 322–9

[75] Müllenbroich M C, Turrini L, Silvestri L, Alterini T, Gheisari A, Tiso N, Vanzi F, Sacconi L and Pavone F S 2018 Bessel Beam Illumination Reduces Random and Systematic Errors in Quantitative Functional Studies Using Light-Sheet Microscopy *Front. Cell. Neurosci.* **12** 315

[76] Sancataldo G, Gavryusev V, de Vito G, Turrini L, Locatelli M, Fornetto C, Tiso N, Vanzi F, Silvestri L and Pavone F S 2019 Flexible Multi-Beam Light-Sheet Fluorescence Microscope for Live Imaging Without Striping Artifacts *Front. Neuroanat.* **13** 7

[77] Gavryusev V, Sancataldo G, Ricci P, Montalbano A, Fornetto C, Turrini L, Laurino A, Pesce L, de Vito G, Tiso N, Vanzi F, Silvestri L and Pavone F S 2019 Dual-beam confocal light-sheet microscopy via flexible acousto-optic deflector *J. Biomed. Opt.* **24** 1

[78] Sancataldo G, Silvestri L, Allegra Mascaro A L, Sacconi L and Pavone F S 2019 Advanced fluorescence microscopy for in vivo imaging of neuronal activity *Optica* **6** 758

[79] Ricci P, Sancataldo G, Gavryusev V, Franceschini A, Müllenbroich M C, Silvestri L and Pavone F S 2020 Fast multi-directional DSLM for confocal detection without striping artifacts *Biomed. Opt. Express* **11** 3111

[80] de Vito G, Turrini L, Fornetto C, Ricci P, Müllenbroich C, Sancataldo G, Trabalzini E, Mazzamuto G, Tiso N, Sacconi L, Fanelli D, Silvestri L, Vanzi F and Pavone F S 2020 Two-photon light-sheet microscopy for high-speed whole-brain functional imaging of zebrafish neuronal physiology and pathology *Neurophotonics* Neurophotonics ed T Kuner, F S Pavone and L Cognet (Online Only, France: SPIE) p 3

[81] de Vito G, Fornetto C, Ricci P, Müllenbroich C, Sancataldo G, Turrini L, Mazzamuto G, Tiso N, Sacconi L, Fanelli D, Silvestri L, Vanzi F and Pavone F S 2020 Two-photon high-speed light-sheet volumetric imaging of brain activity during sleep in zebrafish larvae *Neural Imaging and Sensing 2020* Neural Imaging and Sensing 2020 ed Q Luo, J Ding and L Fu (San Francisco, United States: SPIE) p 3